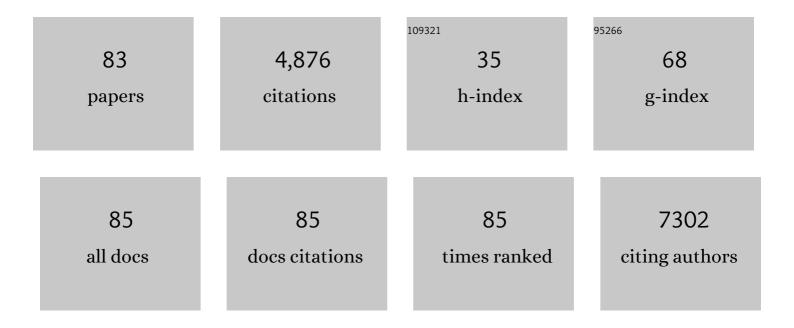
List of Publications by Year in descending order

Source: https://exaly.com/author-pdf/4411795/publications.pdf Version: 2024-02-01



#	Article	IF	CITATIONS
1	Hydrogenation engineering of bimetallic Ag–Cu-modified-titania photocatalysts for production of hydrogen. Catalysis Today, 2022, 388-389, 79-86.	4.4	4
2	Electron transfer dynamics and enhanced H2 production activity of hydrangea-like BiOBr/Bi2S3-based photocatalysts with Cu-complex as a redox mediator. Applied Surface Science, 2022, 576, 151870.	6.1	14
3	Interfacial Engineered Vanadium Oxide Nanoheterostructures Synchronizing High-Energy and Long-Term Potassium-Ion Storage. ACS Nano, 2022, 16, 1502-1510.	14.6	35
4	Interstitial boron-triggered electron-deficient Os aerogels for enhanced pH-universal hydrogen evolution. Nature Communications, 2022, 13, 1143.	12.8	152
5	Extra Storage Capacity Enabled by Structural Defects in Pseudocapacitive NbN Monocrystals for Highâ€Energy Hybrid Supercapacitors. Advanced Functional Materials, 2022, 32, .	14.9	14
6	FeN@N-doped graphitic biochars derived from hydrothermal-microwave pyrolysis of cellulose biomass for fuel cell catalysts. Journal of Analytical and Applied Pyrolysis, 2021, 153, 104991.	5.5	22
7	Ionic liquid/surfactant-hydrothermal synthesis of dendritic PbS@CuS core-shell photocatalysts with improved photocatalytic performance. Applied Surface Science, 2021, 546, 149106.	6.1	26
8	An Efficient Interfacial Synthesis of Twoâ€Đimensional Metal–Organic Framework Nanosheets for Electrochemical Hydrogen Peroxide Production. Angewandte Chemie - International Edition, 2021, 60, 11190-11195.	13.8	89
9	Tailoring the surface oxygen engineering of a carbon-quantum-dot-sensitized ZnO@H-ZnO1-x multijunction toward efficient charge dynamics and photoactivity enhancement. Applied Catalysis B: Environmental, 2021, 285, 119846.	20.2	20
10	Ligandâ€Promoted Cooperative Electrochemical Oxidation of Bioâ€Alcohol on Distorted Cobalt Hydroxides for Bioâ€Hydrogen Extraction. ChemSusChem, 2021, 14, 2612-2620.	6.8	6
11	Microwave solvothermal synthesis of cubic MnS@Ag2S core-shell photocatalysts with improved charge separation and photocatalytic activity. Applied Surface Science, 2021, 558, 149875.	6.1	11
12	Electrosynthesized Ni-P nanospheres with high activity and selectivity towards photoelectrochemical plastics reforming. Applied Catalysis B: Environmental, 2021, 296, 120351.	20.2	41
13	Site-Specified Two-Dimensional Heterojunction of Pt Nanoparticles/Metal–Organic Frameworks for Enhanced Hydrogen Evolution. Journal of the American Chemical Society, 2021, 143, 16512-16518.	13.7	121
14	Synergistic Effects of Plasmonic Gold and Perovskite-Type SrTiO ₃ for Enhanced Photocatalytic Performance of TiO ₂ Nanotube Arrays. Journal of Physical Chemistry C, 2021, 125, 24340-24349.	3.1	10
15	Au-assisted methanol-hydrogenated titanium dioxide for photocatalytic evolution of hydrogen. Catalysis Today, 2020, 358, 143-148.	4.4	3
16	ldentifying the Active Sites of a Single Atom Catalyst with pH-Universal Oxygen Reduction Reaction Activity. Cell Reports Physical Science, 2020, 1, 100115.	5.6	26
17	Carbon-coated porous Si/C composite anode materials via two-step etching/coating processes for lithium-ion batteries. Ceramics International, 2020, 46, 26598-26607.	4.8	22
18	Exploring Lithium Storage Mechanism and Cycling Stability of Bi ₂ Mo ₃ O ₁₂ Binary Metal Oxide Anode Composited with Ti ₃ C ₂ MXene. Batteries and Supercaps, 2020, 3, 1296-1305.	4.7	3

#	Article	IF	CITATIONS
19	Coâ€Induced Electronic Optimization of Hierarchical NiFe LDH for Oxygen Evolution. Small, 2020, 16, e2002426.	10.0	263
20	Nitrogen-Doped Graphene Quantum Dots for Remarkable Solar Hydrogen Production. ACS Applied Energy Materials, 2020, 3, 5322-5332.	5.1	55
21	Synthesis of FeCo–N@N-doped carbon oxygen reduction catalysts <i>via</i> microwave-assisted ammoxidation. Catalysis Science and Technology, 2020, 10, 3949-3958.	4.1	14
22	Tailoring the mesoporous ZnMn2O4 spheres as anode materials with excellent cycle stability for sodium-ion batteries. Journal of Alloys and Compounds, 2020, 844, 156018.	5.5	16
23	KSCN-activation of hydrogenated NiO/TiO2 for enhanced photocatalytic hydrogen evolution. Applied Surface Science, 2020, 511, 145548.	6.1	15
24	Structural and Electronic Optimization of MoS ₂ Edges for Hydrogen Evolution. Journal of the American Chemical Society, 2019, 141, 18578-18584.	13.7	292
25	Two-Dimensional Cobalt Phosphate Hydroxide Nanosheets: A New Type of High-Performance Electrocatalysts with Intrinsic CoO ₆ Lattice Distortion for Water Oxidation. ACS Applied Materials & Interfaces, 2019, 11, 38633-38640.	8.0	31
26	Sandwich-Nanostructured n-Cu ₂ O/AuAg/p-Cu ₂ O Photocathode with Highly Positive Onset Potential for Improved Water Reduction. ACS Applied Materials & Interfaces, 2019, 11, 38625-38632.	8.0	30
27	Effective hydrogenation of TiO2 photocatalysts with CH3OH for enhanced water splitting: A computational and X-ray study. Applied Surface Science, 2019, 488, 546-554.	6.1	11
28	Electrochemical exploration of the effects of calcination temperature of a mesoporous zinc vanadate anode material on the performance of Na-ion batteries. Inorganic Chemistry Frontiers, 2019, 6, 2653-2659.	6.0	22
29	N,P co-coordinated Fe species embedded in carbon hollow spheres for oxygen electrocatalysis. Journal of Materials Chemistry A, 2019, 7, 14732-14742.	10.3	80
30	Study on Optoelectronic Characteristics of ZnGa ₂ O ₄ Thin-Film Phototransistors. ACS Applied Electronic Materials, 2019, 1, 783-788.	4.3	24
31	Highly efficient nitrogen and carbon coordinated N–Co–C electrocatalysts on reduced graphene oxide derived from vitamin-B12 for the hydrogen evolution reaction. Journal of Materials Chemistry A, 2019, 7, 7179-7185.	10.3	41
32	Agl-BiOl-graphene composite photocatalysts with enhanced interfacial charge transfer and photocatalytic H2 production activity. Applied Surface Science, 2019, 469, 703-712.	6.1	58
33	Au@Nb@H x K1-xNbO3 nanopeapods with near-infrared active plasmonic hot-electron injection for water splitting. Nature Communications, 2018, 9, 232.	12.8	55
34	Photocatalytic hydrogen production from glycerol solution at room temperature by ZnO-ZnS/graphene photocatalysts. Applied Surface Science, 2018, 451, 198-206.	6.1	79
35	Preparation and characterization of V-Loaded titania nanotubes for adsorption/photocatalysis of basic dye and environmental hormone contaminated wastewaters. Catalysis Today, 2018, 307, 119-130.	4.4	18
36	Calcium containing iron oxide as an efficient and robust catalyst in (photo-)electrocatalytic water oxidation at neutral pH. Sustainable Energy and Fuels, 2018, 2, 271-279.	4.9	14

#	Article	IF	CITATIONS
37	Biomimicry of Cuscuta electrode design endows hybrid capacitor with ultrahigh energy density exceeding 2 mW h cm ^{â^2} at a power delivery of 25 mW cm ^{â^2} . Journal of Materials Chemistry A, 2017, 5, 4779-4784.	10.3	5
38	Silver nanowires on coffee filter as dual-sensing functionality for efficient and low-cost SERS substrate and electrochemical detection. Sensors and Actuators B: Chemical, 2017, 245, 189-195.	7.8	32
39	Synthesis and characterization of H3PW12O40/Ce0.1Ti0.9O2 for dimethyl carbonate formation via Methanol carbonation. International Journal of Hydrogen Energy, 2017, 42, 22108-22122.	7.1	25
40	Synthesis of Copper Phosphide Nanotube Arrays as Electrodes for Asymmetric Supercapacitors. ACS Sustainable Chemistry and Engineering, 2017, 5, 3863-3870.	6.7	70
41	Synthesis and characterization of magnetic zinc and manganese ferrite catalysts for decomposition of carbon dioxide into methane. International Journal of Hydrogen Energy, 2017, 42, 22123-22137.	7.1	13
42	Room-temperature fabrication of Cu nanobrushes as an effective surface-enhanced Raman scattering substrate. CrystEngComm, 2016, 18, 8284-8290.	2.6	8
43	Electrodeposited Fe 2 TiO 5 nanostructures for photoelectrochemical oxidation of water. Electrochimica Acta, 2016, 213, 898-903.	5.2	20
44	Hierarchical Fe 2 O 3 nanotube/nickel foam electrodes for electrochemical energy storage. Electrochimica Acta, 2016, 216, 287-294.	5.2	25
45	Thermally activated Cu/Cu 2 S/ZnO nanoarchitectures with surface-plasmon-enhanced Raman scattering. Journal of Colloid and Interface Science, 2016, 464, 66-72.	9.4	12
46	Beaded stream-like CoSe ₂ nanoneedle array for efficient hydrogen evolution electrocatalysis. Journal of Materials Chemistry A, 2016, 4, 4553-4561.	10.3	89
47	β-SnWO ₄ Photocatalyst with Controlled Morphological Transition of Cubes to Spikecubes. ACS Catalysis, 2016, 6, 2357-2367.	11.2	29
48	Synthesis of Cu 2 O nanoparticle films at room temperature for solar water splitting. Journal of Colloid and Interface Science, 2016, 471, 76-80.	9.4	17
49	Novel ZnO/Fe ₂ O ₃ Core–Shell Nanowires for Photoelectrochemical Water Splitting. ACS Applied Materials & Interfaces, 2015, 7, 14157-14162.	8.0	175
50	Spontaneous formation of CuO nanosheets on Cu foil for H2O2 detection. Applied Surface Science, 2015, 354, 85-89.	6.1	26
51	Fabrication of homojunction Cu2O solar cells by electrochemical deposition. Applied Surface Science, 2015, 354, 8-13.	6.1	48
52	Silver-decorated hierarchical cuprous oxide micro/nanospheres as highly effective surface-enhanced Raman scattering substrates. Optics Express, 2014, 22, 14617.	3.4	27
53	Hierarchically Porous Calciumâ€containing Manganese Dioxide Nanorod Bundles with Superior Photoelectrochemical Activity. ChemCatChem, 2014, 6, 1684-1690.	3.7	9
54	Photoelectrochemical activity on Ga-polar and N-polar GaN surfaces for energy conversion. Optics Express, 2014, 22, A21.	3.4	26

#	Article	IF	CITATIONS
55	Facile Synthesis of Pt Nanoparticles/ZnO Nanorod Arrays for Photoelectrochemical Water Splitting. Electrochimica Acta, 2014, 120, 1-5.	5.2	38
56	Electrochemical growth and characterization of a p-Cu2O thin film on n-ZnO nanorods for solar cell application. RSC Advances, 2014, 4, 7655.	3.6	28
57	Polarity-dependant Performance of p-Cu2O/n-ZnO Heterojunction Solar Cells. Electrochimica Acta, 2014, 144, 295-299.	5.2	18
58	Cobaltâ€Phosphateâ€Assisted Photoelectrochemical Water Oxidation by Arrays of Molybdenumâ€Doped Zinc Oxide Nanorods. ChemSusChem, 2014, 7, 2748-2754.	6.8	19
59	Synthesis of copper sulfide nanowire arrays for high-performance supercapacitors. Electrochimica Acta, 2014, 139, 401-407.	5.2	163
60	Novel Iron Oxyhydroxide Lepidocrocite Nanosheet as Ultrahigh Power Density Anode Material for Asymmetric Supercapacitors. Small, 2014, 10, 3803-3810.	10.0	143
61	Template synthesis of copper oxide nanowires for photoelectrochemical hydrogen generation. Journal of Electroanalytical Chemistry, 2013, 704, 19-23.	3.8	44
62	Graphene oxide as a promising photocatalyst for CO ₂ to methanol conversion. Nanoscale, 2013, 5, 262-268.	5.6	424
63	Fabrication of coral-like Cu2O nanoelectrode for solar hydrogen generation. Journal of Power Sources, 2013, 242, 541-547.	7.8	82
64	Synthesis of novel Cu2O micro/nanostructural photocathode for solar water splitting. Electrochimica Acta, 2013, 105, 62-68.	5.2	94
65	Direct-growth of poly(3,4-ethylenedioxythiophene) nanowires/carbon cloth as hierarchical supercapacitor electrode in neutral aqueous solution. Journal of Power Sources, 2013, 242, 718-724.	7.8	60
66	Photochemically active reduced graphene oxide with controllable oxidation level. RSC Advances, 2012, 2, 11258.	3.6	22
67	Direct Synthesis of Bimetallic Pd3Ag Nanoalloys from Bulk Pd3Ag Alloy. Inorganic Chemistry, 2012, 51, 13281-13288.	4.0	7
68	Visible-light-driven photocatalytic carbon-doped porous ZnO nanoarchitectures for solar water-splitting. Nanoscale, 2012, 4, 6515.	5.6	126
69	Hierarchical Cu2O photocathodes with nano/microspheres for solar hydrogen generation. RSC Advances, 2012, 2, 12455.	3.6	60
70	Plasmonic Ag@Ag3(PO4)1â^'x nanoparticle photosensitized ZnO nanorod-array photoanodes for water oxidation. Energy and Environmental Science, 2012, 5, 8917.	30.8	103
71	High-cell-voltage supercapacitor of carbon nanotube/carbon cloth operating in neutral aqueous solution. Journal of Materials Chemistry, 2012, 22, 3383.	6.7	126
72	Birnessite-type manganese oxides nanosheets with hole acceptor assisted photoelectrochemical activity in response to visible light. Journal of Materials Chemistry, 2012, 22, 2733-2739.	6.7	89

#	Article	IF	CITATIONS
73	Characteristics and electrochemical performances of lotus-like CuO/Cu(OH)2 hybrid material electrodes. Journal of Electroanalytical Chemistry, 2012, 673, 43-47.	3.8	127
74	Microwave-activated CuO nanotip/ZnO nanorod nanoarchitectures for efficient hydrogen production. Journal of Materials Chemistry, 2011, 21, 324-326.	6.7	46
75	Reversible phase transformation of MnO ₂ nanosheets in an electrochemical capacitor investigated by in situRaman spectroscopy. Chemical Communications, 2011, 47, 1252-1254.	4.1	196
76	One-pot synthesis of CuFeSe2 cuboid nanoparticles. Materials Research Bulletin, 2011, 46, 2117-2119.	5.2	12
77	Polarity-dependent photoelectrochemical activity in ZnO nanostructures for solar water splitting. Electrochemistry Communications, 2011, 13, 1383-1386.	4.7	84
78	Highly flexible supercapacitors with manganese oxide nanosheet/carbon cloth electrode. Electrochimica Acta, 2011, 56, 7124-7130.	5.2	224
79	O2 plasma-activated CuO-ZnO inverse opals as high-performance methanol microreformer. Journal of Materials Chemistry, 2010, 20, 10611.	6.7	21
80	Ternary PtRuNi Nanocatalysts Supported on N-Doped Carbon Nanotubes: Deposition Process, Material Characterization, and Electrochemistry. Journal of the Electrochemical Society, 2009, 156, B1249.	2.9	29
81	Nanostructured Zinc Oxide Nanorods with Copper Nanoparticles as a Microreformation Catalyst. Angewandte Chemie - International Edition, 2009, 48, 7586-7590.	13.8	63
82	Efficient hydrogen production using Cu-based catalysts prepared via homogeneous precipitation. Journal of Materials Chemistry, 2009, 19, 9186.	6.7	16
83	Electrophoretic deposition of PtRu nanoparticles on carbon nanotubes for methanol oxidation. Diamond and Related Materials, 2009, 18, 557-562.	3.9	9